Eur. Phys. J. B **16**, 469–474 (2000)

THE EUROPEAN PHYSICAL JOURNAL B

EDP Sciences

Extension of ferromagnetism and metallicity to electron-rich manganites by Ru-doping: Generation of new CMR oxides $Sm_{0.2}Ca_{0.8}Mn_{1-x}Ru_xO_3$

C. Martin[1,a], A. Maignan[1], M. Hervieu[1], B. Raveau[1], and J. Hejtmanek[2]

[1] Laboratoire CRISMAT[b], ISMRA, 6 boulevard du Maréchal Juin, 14050 Caen Cedex, France
[2] Institute of Physics of ASCR, Cukrovarnicka 10, 16253 Praha 6, Czech Republic

Received 2 March 2000

Abstract. The doping of Mn site with ruthenium, in the n-type manganite $Sm_{0.2}Ca_{0.8}MnO_3$, has been studied using magnetic and transport measurements. We show that Ru induces a ferromagnetic metallic state at low temperature in this Mn^{4+} rich compound, a metal to metal transition replacing the metal to insulator one in the pristine phase. A spectacular increase of T_C up to 240 K is achieved, together with CMR effect. Based on thermoelectric power measurements, we propose that Ru(V) could be at the origin of these exceptional properties, due to ferromagnetic superexchange interactions between Ru(V) and Mn(III), forming in a first step ferromagnetic metallic clusters in the C-type antiferromagnetic insulating matrix.

PACS. 71.30.+h Metal-insulator transitions and other electronic transitions – 75.50.-y Studies of specific magnetic materials – 75.30.Et Exchange and superexchange interactions

1 Introduction

The numerous studies performed these last years on manganese perovskites $Ln_{1-x}A_xMnO_3$ have shown that the colossal magnetoresistance (CMR) effect which appears in these compounds may be the result of subtle competition between ferromagnetism and antiferromagnetism. Recent theoretical calculations which take into account the extended Coulomb interactions suggest that these CMR properties originate from electronic phase separation phenomena [1]. This hypothesis is supported by the experiments performed at low temperature on the $La_{0.5}Ca_{0.5}MnO_3$ CMR manganite which demonstrate the occurrence of a phase separation characterized by the coexistence of ferromagnetic metallic (FMM) and charge-ordered insulating regions [2, 3]. Similarly, for the CMR $Pr_{0.7}Ca_{0.3}MnO_3$ compound, neutron diffraction studies show the coexistence at low temperature of an antiferromagnetic insulating (AFMI) phase reminiscent of the Mn^{3+}: Mn^{4+} 1:1 charge ordering (CO), and of a ferromagnetic metallic (FMM) phase [4]. The electron microscopy images, registered at low temperature for $Pr_{0.7}Ca_{0.3}MnO_3$, reveal the existence of nanoscale FM clusters embedded in a CO-distorted AFM matrix [5]. External perturbations as magnetic field [6], high electric field [7], X-ray [8], electron irradiation [5], chemical pressure [9] have been found to be efficient routes to induce order-disorder and insulator-metal (I-M) transition and consequently CMR in $Pr_{0.7}Ca_{0.3}MnO_3$. More recently, these effects have been interpreted in the framework of the percolation theory [10]. These external actions tend to reduce the size of the CO regions at the benefit of growing FM areas so that the percolation threshold can be crossed through. In this respect, the CO/FM competition inherent to this kind of manganites is an essential ingredient to obtain large CMR effects.

A different attractive manner of inducing the phase separation consists in the controlled doping of Mn-sites by other transition metal cations. Among them, only Cr, Co and Ni were shown to be able to induce an I-M transition [11–13] in $Ln_{0.5}Ca_{0.5}MnO_3$ (Ln = lanthanide) which is the prototype of the CO-AFMI compound. In particular, few percents of Cr substituted for Mn were able to transform the low temperature insulating phase of the $Pr_{1-x}Ca_xMnO_3$ manganites into a semi-metal or a poor metal for $0.33 \leq x \leq 0.55$ [14]. The metallicity results from the induced FM, which was probed by neutron diffraction in $Pr_{0.5}Ca_{0.5}Mn_{0.95}Cr_{0.05}O_3$ [15], such a FM state was not evidenced for substitutions with Mg, Al, Fe, Sn, Ti, Nb, despite their ability to weaken the CO [14, 16]. This difference between the latter and Cr was attributed to the similar electronic configuration $t_{2g}^3 e_g^0$ of Cr^{3+} and Mn^{4+}, which allows a unique magnetic and electronic coupling. Similar effects were observed, more recently with the doping of Mn

[a] e-mail: christine.martin@ismra.fr
[b] UMR 6508 associée au CNRS

sites by ruthenium [17]. But in the latter case, in contrast to chromium doping, a significant increase of T_C with the doping content could be observed in the Ru-doped FMM phase [17,18]. This different behavior of Ru suggests that this element is able to be FM coupled to Mn, whereas Cr and Mn have been shown to be AFM coupled from dichroïsm spectroscopy measurements [19].

Our recent studies of the small A-site cation manganites $Ln_{1-x}Ca_xMnO_3$ [20] have shown the possibility to obtain CMR properties for the n-type region ($x > 0.80$). Nevertheless, the composition range for the appearance of these properties is very narrow. For instance in the system $Sm_{1-y}Ca_yMnO_3$, CMR effect is obtained around $y = 0.85$, but has disappeared for $y = 0.90$ and 0.80 [20]. We believe that Mn-site doping with magnetic cations should be a privilegious method to extend these CMR properties to a larger composition range. In this respect, ruthenium is one of the best candidates due to its ability to exhibit both oxidation states Ru(IV) and Ru(V) [21] whose electronic configurations $t_{2g}^4e_g^0$ and $t_{2g}^3e_g^0$, respectively, should allow ferromagnetic superexchange interaction with Mn(III) ($t_{2g}^3e_g^1$). The ability of Ru to induce ferromagnetism and metallicity in the Mn(IV) rich manganites $Ln_{0.4}Ca_{0.6}MnO_3$ [18] supports this view point. In the present article, we study the substitution of Ru for Mn in the manganite $Sm_{0.2}Ca_{0.8}MnO_3$. The undoped compound exhibits a M-I transition at 150 K. The low temperature phase, below the transition temperature, is monoclinic ($P2_1/m$) and short range ordered tiny domains remain [22]. We show that a metal-metal (M-M) transition can be induced in this phase by Ru doping, together with ferromagnetism below $T_C \sim 170-240$ K, and that CMR can be obtained by tuning the doping level. This suggests once again that FM ruthenium clusters embedded in the AFM matrix are at the origin of the transport and magnetoresistance properties of these materials. The absence of a similar effect with Cr is also discussed.

2 Experimental

The preparation of the $Sm_{0.2}Ca_{0.8}Mn_{1-x}Ru_xO_3$ samples has been reported elsewhere [18], stoichiometric ratio of Sm_2O_3, CaO, MnO_2 and RuO_2 were first heated at 1000 °C, then pressed in the form of bars, sintered at 1500 °C in air with a slow cooling down to 800 °C and quenched to room temperature. The cell parameters have been refined (by using the Fullprof program) from X-ray data, recorded at room temperature with a Philips diffractometer (CuKα radiation). The electron microscopy characterizations (electron diffraction and energy dispersive spectroscopy analysis) were carried out with a JEOL 2010CX electron microscope.

Magnetic properties have been studied by using an AC/DC SQUID magnetometer. Resistivity measurements have been collected by a four-probe technique on ceramic bars. Indium contacts were ultrasonically deposited. A magnetic field ranging from 0 to 7 T was used for the magnetoresistance characterization. The thermoelectric power (S) measurements were carried out with a four-point steady-state method with separated power and measuring contacts. Two differential chromel-constantan thermocouples were used to measure the temperature gradient.

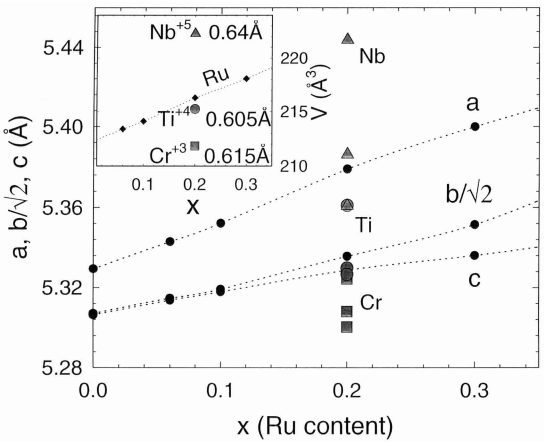

Fig. 1. Cell parameters ($a, b/\sqrt{2}, c$) as a function of x in the $Sm_{0.2}Ca_{0.8}Mn_{1-x}Ru_xO_3$ series (Pnma space group). The cell parameters for 20% Cr^{3+} (gray squares), Ti^{4+} (gray circles) and Nb^{5+} (gray triangles) are also given. The lines are only a guide to the eye. Inset: x dependence of the cell volume (V), the corresponding 20% Cr^{3+}, Ti^{4+} and Nb^{5+} cell volumes are also reported. The labelled cationic sizes are to be compared with those of Mn^{3+} (0.645 Å), Mn^{4+} (0.53 Å), Ru^{3+} (0.68 Å), Ru^{4+} (0.62 Å) and Ru^{5+} (0.565 Å) from reference [31].

3 Results and discussion

The electron diffraction study of $Sm_{0.2}Ca_{0.8}Mn_{0.9}Ru_{0.1}O_3$ shows a Pnma-type structure, from room temperature down to 92 K. The strong monoclinic distortion, observed in the undoped compound [22] and associated with the magnetic transition towards a C-type AFM state, has disappeared in the $Ru_{0.1}$ sample. The absence of twinning domains, which are the signature of the monoclinic distortion in the bright and dark field images, confirms this point. Moreover, the lattice images reveal that there is no short range ordering phenomena occurring in the perovskite matrix, even in the form of tiny domains, unlike the undoped compound. The EDS analyses of the $Ru_{0.1}$ compound confirm, in the limit of accuracy of the technique, the nominal composition and the homogeneity of the sample. For higher doping level, *i.e.* $x = 0.2$, an inhomogeneous cationic distribution appears for the aforementioned thermal process. Nevertheless, the X-ray powder diffraction study, at room temperature, shows a monotonous increase, with x, of the cell volume (inset of Fig. 1) corresponding to an increase of the orthorhombic distortion of the Pnma cell with the Ru content (x), until $x \approx 0.3$ (Fig. 1). Such an evolution is in agreement with a large Mn-valence decrease as x increases, as reported in the $Sm_{1-y}Ca_yMnO_3$ series where we observe a similar tendency for the lattice volume and parameters

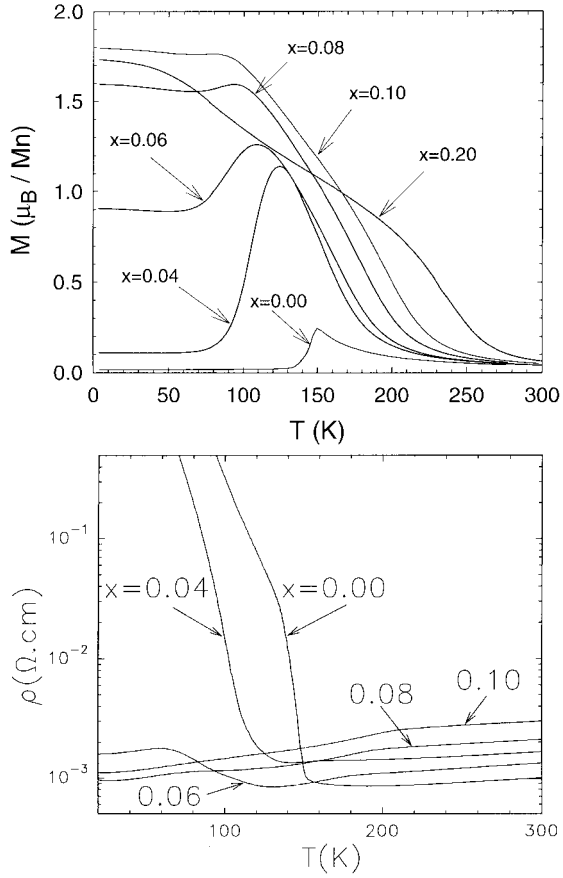

Fig. 2. T dependent magnetization M (a) and resistivity ρ (b) for the $Sm_{0.2}Ca_{0.8}Mn_{1-x}Ru_xO_3$ series. x values are labelled on the graph.

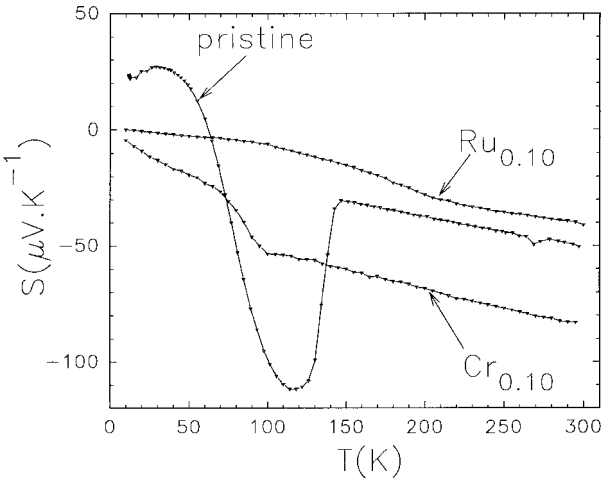

Fig. 3. Thermoelectric power *vs.* T for $Sm_{0.2}Ca_{0.8}MnO_3$, $Sm_{0.2}Ca_{0.8}Mn_{0.9}Ru_{0.1}O_3$ and $Sm_{0.2}Ca_{0.8}Mn_{0.9}Cr_{0.1}O_3$.

as y decreases [22]. The cell parameters also given for samples with 20% of Cr^{3+}, Ti^{4+} or Nb^{5+} for Mn allow to rule out a Ru^{3+} for Mn^{3+} substitution (see the smaller parameters for Cr^{3+}) but, do not allow to distinguish Ru^{4+} from Ru^{5+} (compare the sizes reported in Fig. 1 for the different doping elements).

The magnetization curves of $Sm_{0.2}Ca_{0.8}Mn_{1-x}Ru_xO_3$ for $0 \leq x \leq 0.20$, registered upon heating under 1.4 T after a zero field cooled process, are shown in Figure 2a. The undoped manganite ($x = 0$) shows a transition from PM semimetallic to an AFM C-type insulating state, with $T_N = 150$ K. Note that this transition coincides with a structural transition at T_S from an orthorhombic to monoclinic symmetry, short range ordering being observed concomitantly with the monoclinic phase. As soon as Ru is introduced on the Mn-site, a FMM state is induced, the maximum magnetization (M) value at 4.2 K increasing rapidly from $0.25\,\mu_B$ per mole for $x = 0$ to $1.8\,\mu_B$ for $x = 0.10$. Simultaneously, a clear increase of T_C (taken at the inflection point of the transition) is obtained, reaching 240 K for $x = 0.20$. This extension of the FMM state at the expense of the AFM state is quite remarkable, if one bears in mind that the C-type AFM state is extremely robust and requires a magnetic field higher than 25 T to flip the antiparallel spins [23] in the pristine phase. The high value of T_C is also very striking, compared to the maximum value of 110 K obtained to date in the $Sm_{1-y}Ca_yMnO_3$ system [20,23] for y values close to $y \approx 0.90$.

The $\rho(T)$ curves (Fig. 2b) show that the resistivity at low temperature drops by several orders of magnitude by doping with Ru, ρ decreasing as the Ru content increases. This leads to a metal-metal transition, as soon as $x > 0.04$. As often observed in the perovskite manganites, the metallic character of the low temperature phase is connected with the FM state shown in Figure 2a, so that $T_{MM} \approx T_C$.

Thus, these results show that a FMM state can be induced for the first time in compositions involving average Mn valences much higher than 3.5, by Ru doping. At this point of the investigations, the issue of the ruthenium valence must be discussed, which will indeed influence the manganese valence, due to electroneutrality. Considering the synthesis conditions, in air, two oxidations states are possible for ruthenium, either Ru(IV) as proposed in reference [17], or Ru(V). Results obtained previously by several authors [24], working in air and in double perovskite systems involving strontium, barium or calcium, have definitely shown that for such conditions Ru(V) was the most stable species. Thus we believe that the oxidation state of ruthenium in this doped manganites is mainly pentavalent. Consequently, the introduction of Ru(V) on the Mn-site should increase the Mn(III) content at the expense of the Mn(IV) species, from ($0.8Mn^{4+} + 0.2Mn^{3+}$) for the undoped compound to ($0.6Mn^{4+} + 0.3Mn^{3+} + 0.1Ru^{5+}$) for $x = 0.1$. This hypothesis is compatible with the evolution of the cell parameters reported in Figure 1.

In order to shed light on this problem, thermoelectric power (S) measurements were carried out (Fig. 3). The comparison of the pristine compound, $Sm_{0.8}Ca_{0.2}MnO_3$ [25], with $Sm_{0.8}Ca_{0.2}Mn_{0.9}Ru_{0.1}O_3$ ($x = 0.10$), evidences the dramatic Ru effect upon the electronic properties. For the former, a sharp decrease of S is observed below 150 K which is connected to the strong charge localization occurring at the transition ($T_N \sim T_S$).

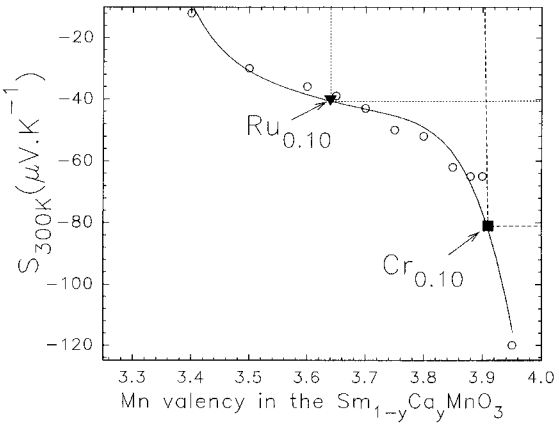

Fig. 4. $S_{300\,\mathrm{K}}$ *vs.* Mn valence from the data obtained for $Sm_{1-y}Ca_yMnO_3$ (from Ref. [25]). The $S_{300\,\mathrm{K}}$ values from Fig. 3 for 10% of Ru and Cr are also given.

In contrast, the $S(T)$ curve of the 10% Ru doped manganite does not exhibit this change below 150 K, but instead a rather smooth curve. A clear change of slope is evidenced at 220 K which is in good coincidence with the T_C determined from Figure 2a and the corresponding M-M transition in Figure 2b. Such a curve shape can be compared to the $S(T)$ curves of Mn^{3+} rich FMM compositions such as $La_{0.6}Ca_{0.4}MnO_3$ [26]. However, the room temperature S value of the Ru doped sample ($S_{300\,\mathrm{K}} = -40\,\mu\mathrm{V\,K^{-1}}$) is much smaller than that of hole doped perovskite manganites [26]. This large negative value confirms the electron-doped character of this manganite. The $S_{300\,\mathrm{K}}$ shifts up from $-50\,\mu\mathrm{V\,K^{-1}}$ to $-40\,\mu\mathrm{V\,K^{-1}}$ as one goes from $Sm_{0.2}Ca_{0.8}MnO_3$ to $Sm_{0.2}Ca_{0.8}Mn_{0.9}Ru_{0.1}O_3$. This is consistent with a decrease of the Mn valence from 3.8 to ~ 3.64 if one refers to the $S_{300\,\mathrm{K}}$ data reported for the $Sm_{1-y}Ca_yMnO_3$ series [25] that are given in Figure 4 where the $S_{300\,\mathrm{K}}$ value of the 10% Ru doped compound is also shown. If Ru^{5+} substitutes Mn, the expected Mn valence for $Sm_{0.2}Ca_{0.8}Mn_{0.9}Ru_{0.1}O_3$ is 3.67 if ruthenium does not participate to the electronic conduction. But if Ru^{5+}, which is isoelectronic to Mn^{4+} (both species are d^3), behaves like a Mn^{4+} cation, this value is 3.70. Both values are close to 3.64 extracted from the $S_{300\,\mathrm{K}}$ (Mn valence) curve established from the $Sm_{1-y}Ca_yMnO_3$ samples (Fig. 4). Most importantly, in both cases, the electron concentration in the ruthenium sample is increased in comparison with that of $Sm_{0.2}Ca_{0.8}MnO_3$, and cannot be attributed to Ru^{4+} (3.78). The ruthenium behavior can be compared to that of another magnetic dopant, isoelectronic to Mn^{4+}, such as trivalent chromium which has been shown to be able to induce FM in $Sm_{0.2}Ca_{0.8}MnO_3$ but no metal to metal transition [27]. In the $Sm_{0.2}Ca_{0.8}Mn_{0.9}Cr_{0.1}O_3$ sample, the theoretical value of the Mn valence is 3.89 ($0.8Mn^{4+} + 0.1Mn^{3+} + 0.1Cr^{3+}$) against 3.90 if Cr^{3+} participates. Those values have to be compared to the 3.90 value obtained in Figure 4 from the $S_{300\,\mathrm{K}} = -81\,\mu\mathrm{V\,K^{-1}}$ value (Fig. 3). Thus, on one hand the Cr substitution tends to increase the Mn average valence so that a FM state is reached below ~ 100 K [27] similar to the FM $Sm_{1-y}Ca_yMnO_3$ compounds with $y \sim 0.9$. On the other hand, tetra and/or pentavalent ruthenium pushes the Mn valence toward Mn^{3+}, *i.e.* Mn valences for which the CO is even more stable. Thus the thermoelectric power observations support the statement that Ru(V) is mainly engaged in the structure, and induces an increase of the Mn^{3+} content. Such a behavior is quite remarkable since it should displace the electron concentration towards smaller y values with respect to the pristine system $Sm_{1-y}Ca_yMnO_3$ (*i.e.* $y < 0.8$), and consequently should reinforce CO (see the corresponding magnetic phase diagram in Ref. [28]). Curiously, we observe the opposite, *i.e.* Ru doping induces a M-M transition, as for $y > 0.8$ compositions. This demonstrates that the valence effect is not the only factor which governs the properties, but that strong FM interactions between Ru(V) and Mn(III) may be prominent with respect to CO, and will be at the origin of the formation of FMM clusters.

Some informations on the origin of the Ru effect can be derived from the observation of the AC-susceptibility (χ', χ'') curves registered with a small ac magnetic field of 3Oe *vs.* T (Fig. 5). As soon as Ru is substituted for Mn, the $\chi'(T)$ curves (Fig. 5a) do not exhibit the unique characteristic transition at T_C of a conventional FM manganite, but a curve characterized by a first peak at $T_C(T_{p1})$ and a broad shoulder below that peak which exhibits a maximum at T_{p2} and a large frequency dependence (Fig. 5b for $x = 0.10$). This kind of curve, with a peak at T_C and large frequency dependence below T_C, is the signature of FM clusters embedded in an AFM matrix as previously reported in the $Ln_{0.1}Ca_{0.9}MnO_3$ manganites [29]. This kind of magnetic behavior is called "cluster-glass" (CG); it was proposed for $La_{1-x}Sr_xCoO_3$ cobaltites which exhibit a competition between FM and AFM interactions responsible for the CG state with short-range FM as the FM exchange interactions overcome the AFM exchange interactions [30]. It is a modified version of the spin-glass (SG) and it can be considered to be a set of clusters, which are short-range ordered near the Curie temperature. Below T_C, the CG exhibits some characteristics features of the SG but with an increased spin density compared to the isolated atomic moments of the SG. One of its signature is a frequency dependence (non-linearity) of the susceptibility below T_C. In this model, it should be pointed out that the effect of Ru doping on the magnetic behavior of the pristine compound $Sm_{0.2}Ca_{0.8}MnO_3$ (inset of Fig. 5a) is dramatic, the χ' maximum value being increased by a factor of ~ 55 with the 4% Ru substitution (Fig. 5a) which confirms the induced ferromagnetism. The first peak at T_C corresponds to the setting of the intracluster FM interactions, which magnitude increases as the Ru content increases since T_C (or T_{p1}) increases (inset of Fig. 5b). These clusters are probably developing around the Ru cations, which tend to create an excess of Mn^{3+} around them. Consequently, islands of Mn^{3+} rich regions with FM coupling between Mn^{3+} and Ru^{5+} coexist within the AFMI Mn^{4+} rich matrix. Increasing the Ru content will tend to make growing these FM areas. The latter develop at the expense of the AFM phase which T_N decreases from

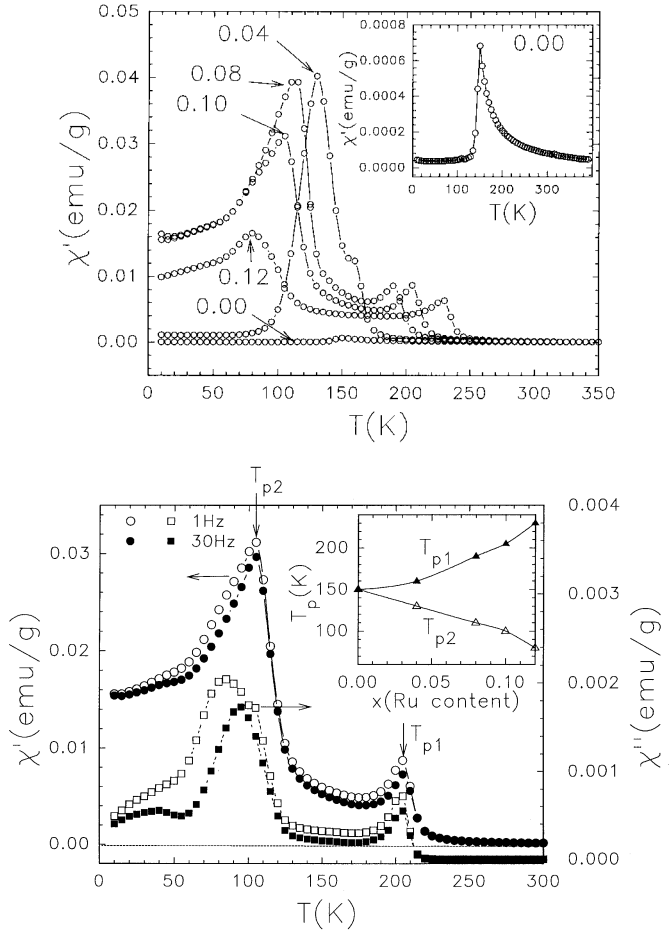

Fig. 5. (a) T dependence of the real part of the ac-susceptibility (χ') of $Sm_{0.2}Ca_{0.8}Mn_{1-x}Ru_xO_3$. Inset: the curve for the $x = 0$ pristine sample is also given. (b) χ'(T) and χ'' (T) curves registered with $f = 1$ and 30 Hz for $Sm_{0.2}Ca_{0.8}Mn_{0.9}Ru_{0.1}O_3$. Inset: x dependence of T_{p1} (T_C) and T_{p2} (T_N).

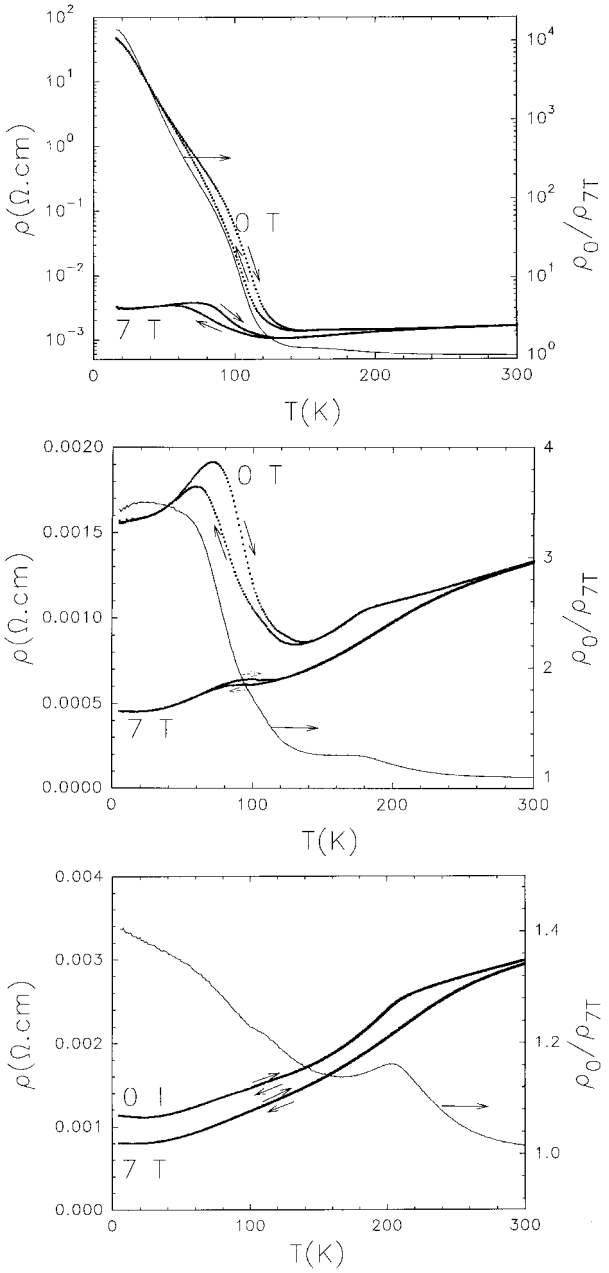

Fig. 6. $\rho(T)$ curves registered upon cooling in and in the absence of magnetic field, $\rho_{7\,T}$ and $\rho_{0\,T}$, respectively. The $\rho_0/\rho_{7\,T}$ ratio is also given (right y-axis). (a) $Sm_{0.2}Ca_{0.8}Mn_{0.96}Ru_{0.04}O_3$; (b) $Sm_{0.2}Ca_{0.8}Mn_{0.94}Ru_{0.06}O_3$ and (c) $Sm_{0.2}Ca_{0.8}Mn_{0.9}Ru_{0.1}O_3$.

150 K for $Sm_{0.2}Ca_{0.8}MnO_3$ (inset of Fig. 5a from Ref. [22]) down to $T_N = T_{p2} = 80$ K for 12% of ruthenium (Fig. 5a and inset of Fig. 5b). In this model, as soon as a percolation path is created, a metallic behavior will be obtained.

This hypothesis is supported by the magnetoresistance curves (Fig. 6). For the larger Ru doping levels, since the samples are metallic at low temperature, the effect of the field on the resistivity (ρ) remains moderate as shown in Figure 6c for $Sm_{0.2}Ca_{0.8}Mn_{0.9}Ru_{0.1}O_3$. On the opposite, for Ru amounts smaller than the percolation concentration, the low temperature resistivity is much higher (lack of percolation) in agreement with the development of the remaining AFMI regions below T_{p2}. The magnetic field application is able to create a percolation path between FM clusters so that a large drop of ρ is induced leading to CMR effects. This is illustrated by the $\rho(T)$ curves obtained for 4% of Ru (Fig. 6a) in 0 and 7 T, from which a resistivity ratio ρ_0/ρ_{7T} of 10^4 is reached at low temperature. It should be pointed out that the highly hysteretic ρ increases at low temperature observed for $x = 0.04$ and $x = 0.06$ (Figs. 6a and 6b) is reminiscent of the structural transition observed at 150 K in $Sm_{0.2}Ca_{0.8}MnO_3$ [22]. As the Ru content increases, the AFMI phase weakens progressively, as shown by the AC-susceptibility curves in Figure 5a, so that for the $x = 0.10$ metallic composition, the percolation threshold is reached (Fig. 6a). This is in agreement with the electron microscopy study performed at 92 K which hardly detects the remaining distorted AFMI phase.

In conclusion, we have shown for the first time the possibility to extend the FMM state of n-type manganites, characterized by small A site cations, towards Mn^{4+} rich compositions, *i.e.* starting from an average manganese valency of 3.8. Moreover we have demonstrated the ability of these n-type manganites to reach high T_C values, larger than 200 K, which were never achieved by chromium doping. These results, and those previously obtained for $Sm_{0.4}Ca_{0.6}Mn_{1-x}Ru_xO_3$ [18], show that ruthenium is a very attractive cation to generate new CMR compounds. They suggest that the FMM state, and consequently the CMR effect, should be extended to a very wide composition range, in the $Sm_{1-y}Ca_yMnO_3$ series, by ruthenium doping. The thermoelectric power measurements support strongly the presence of pentavalent ruthenium, in agreement with previous synthesis made in air for different Ru-based oxides. The simultaneous existence of Ru(IV) and Ru(V), according to the equilibrium Ru(V) + Mn(III) $\leftrightarrow$ Ru(IV) + Mn(IV) cannot, of course, be ruled out. But more important, the present results, and especially the high T_C's, suggest that the FM coupling between Ru(V) and Mn(III), through superexchange, is at the origin of the Ru efficiency.

References

1. A. Moreo, S. Yunoki, E. Dagotto, Science **283**, 2034 (1999).
2. M. Uehara, S. Mori, C. Chen, S.W. Cheong, Nature (London) **399**, 560 (1999).
3. R. Mahendiran, M.R. Ibarra, A. Maignan, C. Martin, B. Raveau, A. Hernando, Solid State Comm. **111**, 525 (1999) and references therein.
4. Z. Jirak, S. Krupicka, Z. Dlouha, S. Vratislav, J. Magn. Magn. Mater. **53**, 153 (1985).
5. M. Hervieu, A. Barnabé, C. Martin, A. Maignan, B. Raveau, Phys. Rev. B **60**, 726 (1999).
6. Y. Tomioka, A. Asamitsu, Y. Moritomo, Y. Tokura, J. Phys. Soc. Jpn **64**, 3626 (1995).
7. A. Asamitsu, Y. Tomioka, H. Kuwahara, Y. Tokura, Nature (London) **388**, 50 (1997).
8. V. Kiryukhin, D. Casa, J.P. Hill, B. Keimer, A. Vigliante, Y. Tomioka, Y. Tokura, Nature (London) **386**, 813 (1997).
9. H.Y. Hwang, S.W. Cheong, D.G. Radaelli, M. Marezio, B. Battlog, Phys. Rev. Lett. **75**, 914 (1995).
10. T. Kimura, Y. Tomioka, R. Kumai, Y. Okimoto, Y. Tokura, Phys. Rev. Lett. **83**, 3940 (1999).
11. B. Raveau, A. Maignan, C. Martin, J. Solid State Chem. **130**, 162 (1997).
12. A. Maignan, F. Damay, C. Martin, B. Raveau, Mat. Res. Bull **32**, 965 (1997).
13. A. Barnabé, A. Maignan, M. Hervieu, F. Damay, C. Martin, B. Raveau, Appl. Phys. Lett. **71**, 3907 (1997).
14. A. Maignan, F. Damay, A. Barnabé, C. Martin, M. Hervieu, B. Raveau, Philos. Trans. Roy. Soc. Lond. A **356**, 1635 (1998).
15. F. Damay, C. Martin, A. Maignan, M. Hervieu, B. Raveau, F. Bourée, G. André, Appl. Phys. Lett. **73**, 3772 (1998).
16. C. Martin, A. Maignan, F. Damay, M. Hervieu, B. Raveau, Z. Jirak, G. André, F. Bourée, J. Magn. Magn. Mater. **202**, 11 (1999).
17. P.V. Vanitha, A. Arulraj, A.R. Raju, C.N.R. Rao, C.R. Acad. Sci. **2**, 595 (1999).
18. B. Raveau, A. Maignan, C. Martin, R. Mahendiran, M. Hervieu, J. Solid State Chem. **151**, 330 (2000).
19. F. Studer, O. Toulemonde, J.B. Goedkoop, A. Barnabé, B. Raveau, Jpn J. Appl. Phys. **38**, 377 (1999).
20. C. Martin, A. Maignan, F. Damay, M. Hervieu, B. Raveau, J. Solid State Chem. **134**, 198 (1997).
21. A. Callaghan, C.W. Moeller, R. Ward, Inorg. Chem. **5**, 1572 (1966).
22. M. Hervieu, A. Barnabé, C. Martin, A. Maignan, F. Damay, B. Raveau, Eur. Phys. J. B **8**, 31 (1999).
23. M. Respaud, C. Martin, A. Maignan, M. Hervieu, B. Raveau, *Proceeding of 18th General Conference of the Condensed Matter Division of Eur. Phys. Soc. Montreux, Switzerland, 13-17 March 2000*, p. 204.
24. P.D. Battle, C.W. Jones, J. Solid State Chem. **78**, 108 (1989); P.D. Battle, T.C. Gibb, C.W. Jones, F. Studer, *ibid.* **78**, 281 (1989); P.D. Battle, C.W. Jones, F. Studer, *ibid.* **90**, 302 (1991).
25. J. Hejtmanek, Z. Jirak, M. Marysko, C. Martin, A. Maignan, M. Hervieu, B. Raveau, Phys. Rev. B **60**, 14057 (1999).
26. M. F. Hundley, J.J. Newmeier, Phys. Rev. B **55**, 11511 (1997).
27. A. Maignan, C. Martin, F. Damay, M. Hervieu, B. Raveau, J. Magn. Magn. Mater **188**, 185 (1998).
28. C. Martin, A. Maignan, M. Hervieu, B. Raveau, Phys. Rev. B **60**, 12191 (1999).
29. A. Maignan, C. Martin, F. Damay, B. Raveau, J. Hejtmanek, Phys. Rev. B **58**, 2758 (1998).
30. S. Mukherjee, R. Ranganathan, P.S. Anilkumar, P.A. Joy, Phys. Rev. B **54**, 9267 (1996).
31. R.D. Shannon, Acta Cryst. A **32**, 751 (1976).